

Generation and Propagation Characteristics Analysis through Atmosphere of Gaussian-Bessel-correlated Schell-model Beam

Zeyu Zhou¹, Xiuhua Yuan^{*1}, Wei Yao²

1: School of Optical and Electronic Information, Huazhong University of Science and Technology, Wuhan China

2: Shenzhen Research Institution, Huazhong University of Science and Technology, Shenzhen, China

Email: *yuanxh@hust.edu.cn, zhouzeyu@hust.edu.cn, yaowei@163.com

Abstract—In this paper, propagation characteristics of Gaussian-Bessel-correlated Schell-model beam (GBSM) in turbulent atmosphere have been studied through simulation and experimentation. Without studying its quality in communication directly, we use scintillation index (SI) and beam expansion to estimate such beams as signal lights. We use Monte-Carlo method to generate the phase screen for modeling the atmosphere in simulation. An experiment consisting of a phase-only spatial light modulator (SLM) and a rotating ground-glass disk (RGGD) is used to generate a GBSM beam. A box with fans and heaters inside creates a real, but much stronger, turbulent atmosphere environment along the propagation path. Comparing to other kinds of beams, like conventional Gaussian Schell-model beam (GSM), GBSM has a faster speed of beam expansion and better fluctuation characteristics in far propagation range while GSM and GBSM have the same initial coherence radius.

Keywords- GBSM; generation; turbulence; propagation.

I. INTRODUCTION

Since the appearance of the laser, it has been used in fields of communication, detection, illumination, imaging and even in military for its advantages in coherence and orientation. However, influenced by atmospheric turbulence, especially near the ground, the front wave of the beam breaks and the beam intensity fluctuates, which limits the usage of laser in atmosphere. Since Ronald Fante [1] proved in 1981 that a partially coherent beam has extreme improvement on the intensity fluctuation, people have studied many kinds of beams with different coherence profiles. Besides the conventional Gaussian Schell-model beams (GSB) [2], beams with non-Gaussian coherence degree like pseudo-Bessel-correlated beams (PBCB) [3], multiple Gaussian Schell-model beams (MGSB) [4], Laguerre-Gaussian Schell-model beams (LGSB) [5], rectangular Gaussian Schell-model beams [6] have also been studied in turbulence.

All of such beams with spatial partial coherence are better than coherent Gaussian beam with respect to the scintillation index. Moreover, the lower the coherence degree, the lower the SI. Since so many achievements have come out in this field, scintillation of GBSM still remains its value for study. Thus, we want to further compensate this work.

The rest of the paper is structured as follows. In Section 2, a method to generate GBSM is introduced in theory and tested in an experiment. Afterwards, the average intensity distribution of GBSM beam is deduced theoretically, and the intensity fluctuation quality is analyzed via simulation in Section 3. We conclude the paper in Section 4.

II. GENERATION OF GBSM

A. Gaussian-Bessel-correlated Schell-model beam

The GBSM is a partially coherent beam with non-conventional correlation form defined by Gaussian-Bessel function. Even though it has stochastic field, the GBSM can be described by auto-correlation function, a second-order moment of optical field $U(r)$, as (1)

$$\langle U(\vec{r}_1)U^*(\vec{r}_2) \rangle = \langle U(\vec{r}_1) \rangle \langle U^*(\vec{r}_2) \rangle J_0 \left(\frac{|\vec{r}_1 - \vec{r}_2|}{\alpha} \right) \exp \left(- \frac{|\vec{r}_1 - \vec{r}_2|^2}{\beta^2} \right), \quad (1)$$

where the superscript asterisk means conjugation of the field, and the angular bracket means ensemble average. J_0 here means the first kind of Bessel function on zero-order. α is the parameter controlling the Bessel component, and β determines the truncation width of exponential function.

To generate such a beam, we use a Kepler telescope structure with a RGGD [7] placed on the common focus of two lenses, see Figure 1. When a Gaussian-Bessel beam,

$$U(\vec{s}) = J_0 \left(\frac{|\vec{s}|}{\alpha_0} \right) \exp \left(- \frac{s^2}{\beta_0^2} \right) \quad (2)$$

where \vec{s} is a vector which describe the location of arbitrary field point on plane in front of the first lens f_1 , illuminates the first lens of the telescope, there will appear an annular beam spot on the RGGD. Assuming the field through the RGGD becomes totally incoherent, we can consider the field behind RGGD as a random field which obeys δ distribution,

$$M(\vec{t}_1, \vec{t}_2) = \langle U(\vec{t}_1)U^*(\vec{t}_2) \rangle = \sqrt{I(\vec{t}_1)I(\vec{t}_2)}\delta(\vec{t}_1, \vec{t}_2) \quad (3)$$

where $I(t)$ means the beam intensity on point t ,

$$I(\vec{t}) = U(\vec{t})U^*(\vec{t}). \quad (4)$$

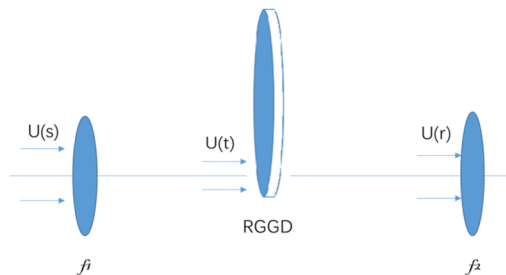


Figure 1. GBSM beam generation illustration

With Fresnel diffraction theory, we can find optical field $U(t)$ in (4) is Fourier transformation of $U(s)$ in (2). It has the convolution between an annular impulse and a Gaussian function

$$U(\vec{t}) \propto \exp\left(\frac{ik}{2f_1} t^2\right) \delta\left(|\vec{t}| - \frac{\lambda f_1}{2\pi\alpha_0}\right) * \exp\left(-\frac{\pi^2 \beta_0^2 t^2}{\lambda^2 f_1^2}\right). \quad (5)$$

When α is far smaller than β , we can consider that $I(t)$ becomes a convolution between square of two parts as (6)

$$I(\vec{t}) \propto \delta\left(|\vec{t}| - \frac{\lambda f_1}{2\pi\alpha_0}\right) * \exp\left(-\frac{2\pi^2 \beta_0^2 t^2}{\lambda^2 f_1^2}\right). \quad (6)$$

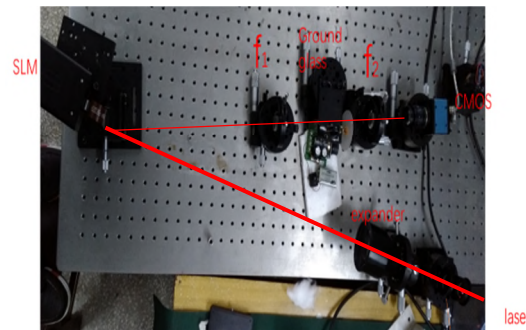
After passing through the second lens f_2 , the auto-correlation function of $U(r)$ can be obtained,

$$\begin{aligned} \langle U(\vec{r}_1) U^*(\vec{r}_2) \rangle &= \left(\frac{k}{2\pi f_2}\right)^2 \iint_{-\infty}^{\infty} d^2 t_1 \iint_{-\infty}^{\infty} d^2 t_2 M(\vec{t}_1, \vec{t}_2) \\ &\times \exp\left[\frac{ik}{2f_2} |\vec{t}_1 - \vec{r}_1|^2 - \frac{ik}{2f_2} |\vec{t}_2 - \vec{r}_2|^2\right] \exp\left(-\frac{ik}{2f_2} r_1^2 + \frac{ik}{2f_2} r_2^2\right) \\ &= \left(\frac{k}{2\pi f_2}\right)^2 \iint_{-\infty}^{\infty} d^2 t I(\vec{t}) \exp\left[\frac{ik}{f_2} (\vec{r}_1 - \vec{r}_2) \cdot \vec{t}\right] \\ &\propto J_0\left(\frac{f_1 |\vec{r}_1 - \vec{r}_2|}{f_2 \alpha_0}\right) \exp\left(-\frac{f_1^2 |\vec{r}_1 - \vec{r}_2|^2}{2f_2^2 \beta_0^2}\right) \end{aligned} \quad (7)$$

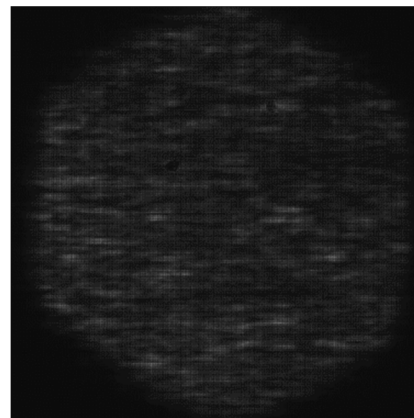
In the deduction of (7), considering the integration in the third line is, mathematically, a Fourier transformation of $I(t)$ which is represented in (6), it is convenient to derive to the last result by multiplying the Fourier transformations of each part in convolution of $I(t)$. By changing the parameters of the incident beam, we can adjust the coherence quality conveniently.

B. Generation of GBSM in experiment

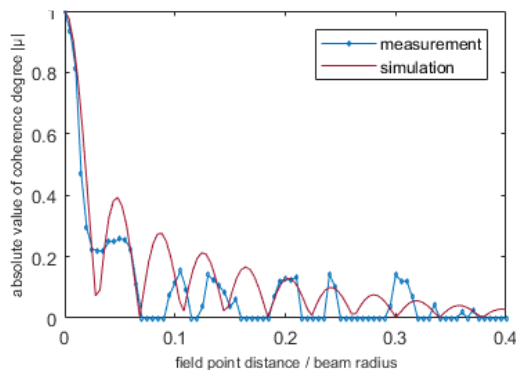
From Figure 1, we establish an experiment structure to generate a GBSM beam, which is presented in Figure 2. We use He-Ne laser (632.8nm) as the laser source. Phase-only SLM (HOLOEYE PLUTO) is used instead of an axicon to generate a Gaussian-Bessel beam. After passing through the telescope structure with RGGD, a partially coherent beam comes out. As the glass is using 320 mesh quartz sand to grind, the RGGD has a coherent length of about 80um, making every 1mm² illumination area include about 150 coherent units, which can be regarded to meet the demand for δ distribution. The RGGD has a diameter of 60mm, when the optical axis is 20mm from the disk center, and illumination area about 2mm², rotation speed adjusted to


 Figure 2. Experiment illustration of GBSM generation. SLM: spatial light modulator. f_1 , f_2 : lenses with focus length of f_1 and f_2 respectively. Laser: 632.8nm He-Ne laser

1r/s, the coherent time of the beam will be fixed at about 50us. To observe this beam, we use a CMOS with exposure time of 200us. The beam in CMOS is presented in Figure 3(a). According to Gaussian momentum theory [8], we calculate the coherence degree of optical field through count the intensity variation from 2000 pictures and finally print it in Figure 3(b). Even though the graph is not excellently matching the expectation, we can still tell the tendency of Gaussian-Bessel function. Many factors lead to this deviation. The Bessel-Gaussian beam created after SLM is not accurate enough. Crosstalk between the fringes exists. Furthermore, coherence length of RGGD is still too large to



(a)



(b)

Figure 3. Generation of GBSM, (a) is the picture of a sample from CMOS and (b) is the curve graph of coherence degree varying with the field point distance relative to beam radius

form the δ distribution, which makes the coherence degree out of its shape. Also, because of the improper set of axis, we miss the details and since the interval between each pixel on the CMOS is limited, it is unavailable for us to adjust the axis setting to a proper one.

III. PROPAGATION CHARACTERISTICS OF GBSM

A. Average intensity of GBSM in atmospheric turbulence

The extended Huygens-Fresnel theory has the advantage to calculate such complex random optic field. As compared to the Rytov approximation, this method avoids to deduce the first and second order perturbation from turbulence to optic field, which is difficult and worthless. This theory divides the entire field into countless spherical secondary sources, and the influence from randomly varying refractive on the wave front can be described by the widely acceptable complex phase perturbation factor for spherical wave.

The atmospheric turbulence is described by turbulence eddies and turbulence influences the beam propagation by randomly changing reflective index. We deem that the reflective index $n(R)$ has a spatial power spectrum

$$\Phi_n(\kappa) = 0.033C_n^2\kappa^{-11/3}\exp\left(-\frac{\kappa^2}{\kappa_l^2}\right) \quad (8)$$

which is named Tatarskii spectrum. C_n^2 is refractive index structure constant used to describe the fluctuation intensity of turbulence. $\kappa_l = \frac{5.92}{l_0}$ represents the spatial frequency of inner scale l_0 . Utilizing extended Huygens-Fresnel theory, the average intensity of beam after propagating a length of L in atmospheric turbulence can be written as

$$I(\vec{\rho}, L) = \left(\frac{k}{2\pi L}\right)^2 \iint_{-\infty}^{\infty} \iint_{-\infty}^{\infty} d^2r_1 d^2r_2 \langle U(\vec{r}_1, 0)U^*(\vec{r}_2, 0) \rangle \times \exp\left[\frac{ik}{2L}|\vec{r}_1 - \vec{\rho}|^2 - \frac{ik}{2L}|\vec{r}_2 - \vec{\rho}|^2\right] \langle \exp[\phi(\vec{\rho}, \vec{r}_1) + \phi^*(\vec{\rho}, \vec{r}_2)] \rangle \quad (9)$$

where ϕ stands for the additional phase from the turbulence eddies through which the beam passes. We have assumed the stochastic behavior of optic source and that of refractive distribution are stochastically independent. The part in angular bracket can be written as [9]

$$\langle \exp[\phi(\vec{\rho}, \vec{r}_1) + \phi^*(\vec{\rho}, \vec{r}_2)] \rangle \approx -0.145C_n^2k^2L\kappa_l^{1/3}Q^2 \quad (10)$$

where we use an algebraic substitution

$$\vec{Q} = \vec{r}_1 - \vec{r}_2. \quad (11)$$

If we also make

$$\vec{R} = \frac{1}{2}(\vec{r}_1 + \vec{r}_2) \quad (12)$$

and substitute (1) and (10-11) into (9), after integrating, the average intensity turn into a convolution

$$I(\vec{\rho}, L) \propto \delta(|\vec{\rho}| - T) * \exp\left(-\frac{\rho^2}{w^2}\right), \quad (13)$$

where

$$T = \frac{L}{2\pi\alpha k} \quad (14)$$

is the radius of annular beam profile, and

$$w^2 = \frac{2\pi^2L^2}{k^2w_0^2} + \frac{\pi^2w_0^2}{2} + \frac{4\pi^2L^2}{k^2\beta^2} + 5.724C_n^2k^2L^3\kappa_l^{1/3} \quad (15)$$

is the beam expansion which result from free space diffraction and turbulence fluctuation. Through (14) and

(15), we can see the radius of annular beam profile has nothing to do with turbulence fluctuation. Apart from propagation length and wavelength, only the parameter of Bessel function part has the ability to determine the ring's radius. Since the inner scale l_0 is in the magnitude of millimeter, when it is in short propagation length, the second part of (15) is the majority determines the beam radius, instead of the part associated with β . Hence, the ring profile cannot be observed if $T < w$, or

$$\alpha > \frac{L}{\sqrt{2\pi^2kw_0}}. \quad (16)$$

Making α reach to infinity, Eq. (13) reduces to the intensity distribution of GSM. Beam expansion (15) becomes beam radius

$$w_G^2 = \frac{2\pi^2L^2}{k^2w_0^2} + \frac{\pi^2w_0^2}{2} + \frac{4\pi^2L^2}{k^2\beta^2} + 5.724C_n^2k^2L^3\kappa_l^{1/3}. \quad (17)$$

Compared to GSM, the GBSM beam, with a same coherence length, obviously has a larger beam expansion. However, if the hollow profile becomes useful, the GBSM beam may have advantage over GSM.

B. Scintillation index

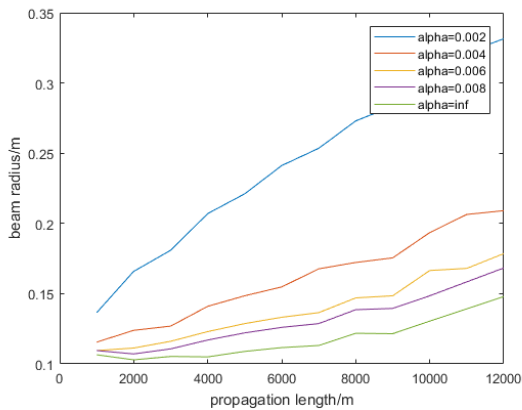
Even though we have given out the average intensity of beam after propagating through turbulence, we have no idea how the intensity fluctuation is. The Monte-Carlo method helps us create a phase screen through which the optical beam will get a randomly changing phase factor. This phase factor represents the influence of turbulence on the laser beam. In order to reduce the simulation error, the propagation of laser beam is devised into several parts. For each part, the angular spectrum method is used to calculate the output field.

The scintillation index is a normalized variance of intensity, which is used to estimate the intensity fluctuation of the laser beam. SI is defined as below,

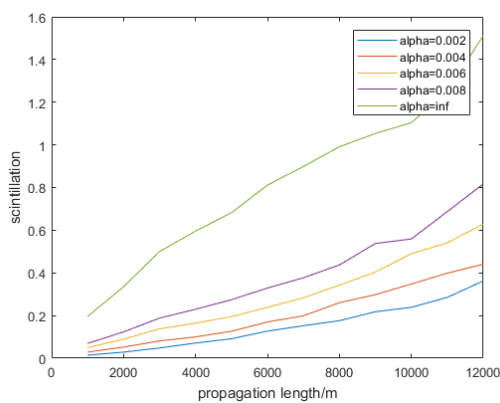
$$\sigma_I^2 = \frac{\langle I^2 \rangle}{\langle I \rangle^2} - 1. \quad (18)$$

For a communication application, a low intensity fluctuation is of much expectation. Because the receiver always has an effective area, leading to a so called aperture averaging, analyzing the total energy fluctuation on a fixed area is more helpful. And, since both the optical field and the channel media have random characteristics, a large number of samples are necessary. After about 2000 realizations, the statistical result becomes stable.

First, we check the impact of Bessel parameter on the scintillation index. We make α vary from 0.002m to infinite at which the light becomes GSM. Gaussian parameter β is fixed on the value of 0.05m. Detection diameter is set to 50mm. Their scintillation indices on the observation plane, which is placed several different distances away from transmission plane, are presented in Figure 4(a). Same as our recognition of relationship between scintillation and beam coherence degree, the SI decreases with the beam coherence length which, in this case, is determined by α , except the infinite one by β . Figure 4(b) is the responding beam radius variation, which is contrary to SI.



(a)



(b)

Figure 4. Scintillation indices (a) and beam radius (b) of GBSM beams with different Bessel parameter α of 0.002, 0.004, 0.006, 0.008, infinite varying with propagation length

Even though we have studied the effect of coherence parameter, the profile of coherence degree distribution is still of much importance. As conventional GSM beam has already proved to be better than coherent Gaussian beam,

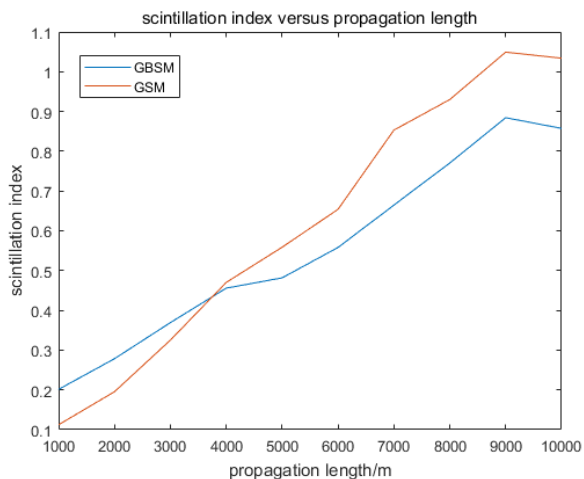
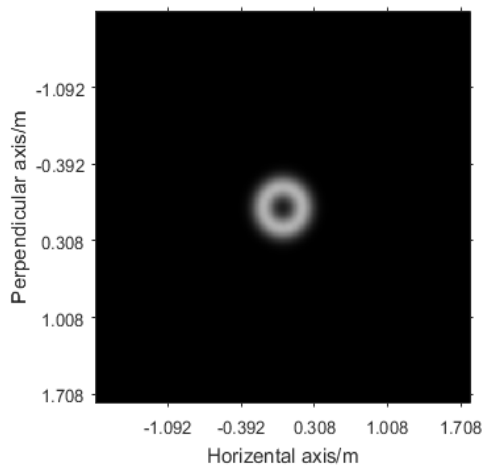
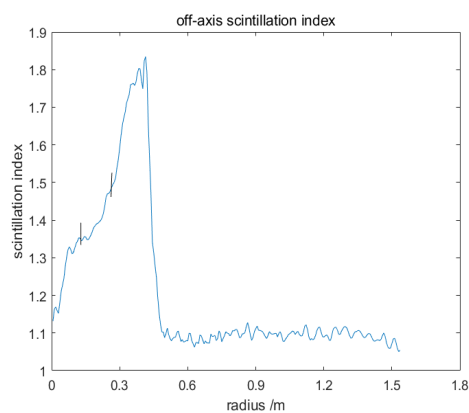


Figure 5. Scintillation indices of GBSM and GSM with the same coherence length of 3.5mm versus propagation length



(a)



(b)

Figure 6. Intensity distribution (a) and off-axis scintillation (b) of GBSM with Bessel parameter of 0.001 after propagating 6km in turbulence

we use GSM only to compare with GBSM beam. In this simulation, the laser wavelength is 1.55 μm . Coherence length and beam width is fixed to about 3.5 mm and 14 cm, respectively. The result of the scintillation index on the detection area of such two kinds of beams varying with propagation length is presented in Figure 5. According to the result, obviously, the GBSM beam has a larger on-axis scintillation in a short range, but it becomes the smaller one in the long range. The reason of this result is unclear. There is only a surmise of it, which is based on the evolution of intensity distribution of GBSM. As the ring-like profile this beam has in a short range, even it may be blurry when the ring's radius is less than the Gaussian expansion, the lower level of average energy distribution on the center point leads to a larger relative fluctuation. With the further propagation of the beam, the ring of GBSM diffuses, but slowly comparing to GSM, which making more energy left in the center area. This may control the scintillation increasing slowly.

In the last part, we determined the optical intensity distribution. We saw the beam profile would become a hollow. It is of considerable need to research the off-axis SI. According to (16), setting α to be 0.001m and β still 0.05m, after 6km propagation, the beam profile and off-axis scintillation index is presented in Figure 6. The interval in Figure 6(b) between two vertical lines corresponds to the ring part of profile in Figure 6(a). There are two rapid rises separated by the ring area. Without theoretical analysis, the reason why it happens is unclear.

IV. CONCLUSION

In this paper, we have analyzed the average intensity and scintillation index of GBSM. Compared to GSM, it has an annular intensity profile, leading a larger beam intensity distribution. However, the radius of the annular profile is fixed by Bessel parameter and propagation length, making the beam somewhat controllable and practical. Its scintillation index is lower over a long distance, but rapid rise of scintillation index off the axis likely causes the application limitation of GBSM. We have generated a GBSM beam using a SLM and an RGGD. The result seems acceptable.

Next, we plan to use this beam as a communication light source, testing its application in communication. Since the partial coherence of beam leads to intensity fluctuation even in initial plan of beam propagation, but there is a time average process when the beam is used in communication, so it is necessary to analyze the influence from coherence time of the source, observer and random media on scintillation index.

ACKNOWLEDGMENT

This research is supported by Shenzhen Research Institution of Huazhong University of Science and Technology.

REFERENCES

- [1] R. L. Fante, "Intensity Fluctuations of an Optical Wave in a Turbulent Medium Effect of Source Coherence," *Optica Acta*, vol. 28, no. 9, pp. 1203-1207, 1981.
- [2] G. Gbur and E. Wolf, "Spreading of partially coherent beams in random media," *J. Opt. Soc. Am. A*, vol. 19, no. 8, pp. 1592-1598, 2002.
- [3] Y. Gu and G. Gbur, "Scintillation of pseudo-Bessel correlated beams in atmospheric turbulence," *J. Opt. Soc. Am. A*, vol. 27, no. 12, pp. 2621-2629, 2010.
- [4] Y. Yuan and Y. Cai, "Scintillation index of a multi-Gaussian Schell-model beam in turbulent atmosphere," *Optics Communications*, vol. 305, pp. 57-65, 2013.
- [5] R. Chen et al, "Statistical properties of a Laguerre-Gaussian Schell-model beam in turbulent atmosphere," *Optics Express*, vol. 22, no. 2 pp. 1871-1883, 2014.
- [6] O. Korotkova and E. Shchepakina, "Rectangular Multi-Gaussian Schell-Model beams in atmospheric turbulence," *Journal of Optics*, vol. 16, no. 4, pp. 1-8, 2014.
- [7] Y. Cai, Y. Chen and F. Wang, "Generation and propagation of partially coherent beams with nonconventional correlation functions: a review [Invited]," *J. Opt. Soc. Am. A*, vol. 31, no. 9, pp. 2083-2096, 2014.
- [8] L. Mandel and E. Wolf, "Coherence and Quantum Optics," Cambridge: Cambridge University Press, 2001.
- [9] L. C. Andrews and R. L. Phillips, "Laser beam propagation through random medium," SPIE Press, 1998.